REMBRANDT IMPACT BASIN ON MERCURY: DETERMINING THE ORIGIN OF LOW- AND HIGH-ALBEDO SMOOTH PLAINS.

J. L. Whitten[1] and J. W. Head[2], [1]Center for Earth and Planetary Studies, Smithsonian Institution, MRC 315, PO Box 37012, Washington, DC 20013-7012 (WhittenJ@si.edu), [2]Dept. of Earth, Environmental and Planetary Sciences, Brown University, Providence, RI 02912.

Introduction: Rembrandt impact basin (~715 km in diameter) is one the largest and most well-preserved impact basins on Mercury [1]. Crater density measurements indicate that Rembrandt is comparable in age to the Caloris impact basin, the largest and also one of the youngest basins on Mercury [e.g., 2, 3]. The basin rim-crest is visible and several massifs define an inner ring approximately 450 km in diameter. A second inner ring is suggested by a circle of wrinkle ridges in the innermost part of the impact basin [2].

Rembrandt basin is both surrounded by and contains smooth plains deposits of varying albedo. This observation has been made using the MErcury Surface, Space ENvironment, GEochemistry and Ranging (MESSENGER) Mercury Atmospheric and Surface Composition Spectrometer (MASCS) and Mercury Dual Imaging System (MDIS) datasets [4-6]. Like most of the impact basins on Mercury, Rembrandt is filled with and surrounded by HRP [7] smooth plains which are interpreted to be formed volcanically [8]. However, low-albedo plains can also be found within and around the exterior of Rembrandt. This low-albedo material is classified as low-reflectance material (LRM [7]) and has been found around several other large impact basins including Tolstoj and Caloris; this LRM material is interpreted to be excavated lower crustal or upper mantle material [9].

Most of the plains deposits on Mercury have been interpreted as volcanic, including the smooth plains (i.e. HRP) [7, 8] and the intercrater plains [e.g., 10]. However, as exemplified by deposits on the Moon, smooth plains can also form by impact related processes, either as ponded impact melt or fluidized impact ejecta [e.g., 11]. Impact melt scaling laws indicate that impacts on Mercury should produce proportionally more impact melt [12], but there is little conclusive evidence for extensive impact melt deposits around large impact basins. The variable albedo of smooth plains around Rembrandt basin inspired us to assess the importance of basin impact melt on the surface modification of Mercury. Specific questions to address include: Are there different types of smooth plains deposits around Rembrandt? Are all of the smooth plains formed by the same process? If so, are the plains formed volcanically or by impact-related processes? What was the sequence of geologic events at Rembrandt impact basin?

Methods: The MESSENGER MDIS dataset was used in this study to map and characterize the smooth plains within and around Rembrandt basin. The boundaries of the different smooth plains deposits were mapped using both an MDIS 750 nm albedo mosaic and a high-incidence angle map. The high-incidence angle map was helpful in discerning the texture of surfaces because the low sun angle creates long shadows that accentuate the morphology of lower slopes and smaller surface features. Areal crater density values, reported as $N(20)$ [13], for each of the defined plains units were calculated to determine the relative stratigraphy of smooth plains deposits and the impact basin formation event. Superposed craters >5 km in diameter were counted to determine the areal crater density values of the smooth plains deposits and basin materials. Embayed craters were used to estimate the volume of the smooth plains deposits using crater morphologic relationships [14, 15]. The reflectance of the different smooth plains units was measured using the 1000 nm wavelength channel from the 8-band MDIS color dataset. MDIS data were supplemented by stereo photogrammetric topography data [16, 17] to measure the average elevations of the mapped smooth plains deposits.

Results: Two different smooth plains deposits were identified around Rembrandt (Fig. 1), the low-albedo plains (LAP) and the high-albedo plains (HAP). LAP are confined to the southwestern half of the basin exterior and tend to be associated with both high and low elevations. HAP almost completely fill the basin interior and topographic lows (e.g., impact craters) exterior to Rembrandt.

*Crater density values (N(*20*))*: HAP are the youngest materials; the exterior HAP are the youngest ($N(20)=11\pm11$), followed by the interior HAP (38±13). The Rembrandt formation event and the LAP have the same crater density value within error (58±16 and 53±13, respectively).

Surface reflectance (1000 nm): HAP share the same reflectance properties as the HRP [7] and the LAP albedo values fall between intermediate plains (IP [7]) and low-reflectance blue plains (LBP, [7]).

Volume estimates of exterior plains: HAP (Unit 1, Fig. 1) are 3.54×10^4 km^3, while LAP vary between 2.01×10^4 and 1.08×10^5 km^3 (Units 2-5, Fig. 1).

Discussion/ Conclusions: The HAP, interior and exterior, are consistent with HRP and are interpreted as volcanic in origin based on a high albedo, low areal crater density, concentration in topographic lows, smooth surface texture, and embayment relationships.

The LAP are interpreted as impact-related melt deposits due to the high density of superposed craters (similar to the basin crater density) and a low surface reflectance; both are characteristics shared with Rembrandt rim materials (which are interpreted to represent excavated pre-basin target material), and are also consistent with ejecta deposits around other impact basin ejecta deposits such as Tolstoj [7, 9]. Impact melt scaling relationships [12] indicate that the total volume of LAP is consistent with the amount of impact melt expected exterior to a basin the size of Rembrandt. Additionally, the distribution of the low-albedo plains (immediately adjacent to and on the Rembrandt basin rim-crest) supports an impact melt origin.

References: [1] Fassett C.I. et al. (2012) *JGR*, 117, E00L08. [2] Watters T.R. et al. (2009) *Science*, 324, 618−621. [3] Whitten J.L. & Head J.W. (2014) *Icarus*, submitted. [4] Helbert J. et al. (2013) *LPSC*, 44, abstract 1496. [5] Izenberg N.R. (2014) *Icarus*, 228, 364−374. [6] D'Amore M. et al. (2014) *LPSC*, 45, abstract 1073. [7] Denevi B.W. et al. (2009) *Science*, 324, 613−618. [8] Denevi B.W. et al. (2013) *JGR*, 118, 891−907. [9] Ernst C.M. et al. (2014) *Icarus*, in press. [10] Whitten J.L. et al. (2014) *Icarus*, 241, 97−113. [11] Oberbeck V.R. et al. (1977) JGR, 82, 1681−1698. [12] Cintala M.J. & Grieve R.A.F. (1998) *MAPS*, 33, 889−912. [13] Crater Analysis Techniques Working Group (1979) *Icarus* 37, 467–474. [14] Pike R.J. (1988) *Mercury*, Univ. Ariz. Press, 165−273. [15] Barnouin O.S. et al. (2012) *Icarus*, 219, 414−427. [16] Gaskell R.W. et al. (2008) *AAS Division Planet. Sci. Meeting*, 40, Abstract #51.05. [17] Edmundson K.L. et al (2011) *GSA Abstracts with Programs* 43 (5), paper 100-6, p. 267.

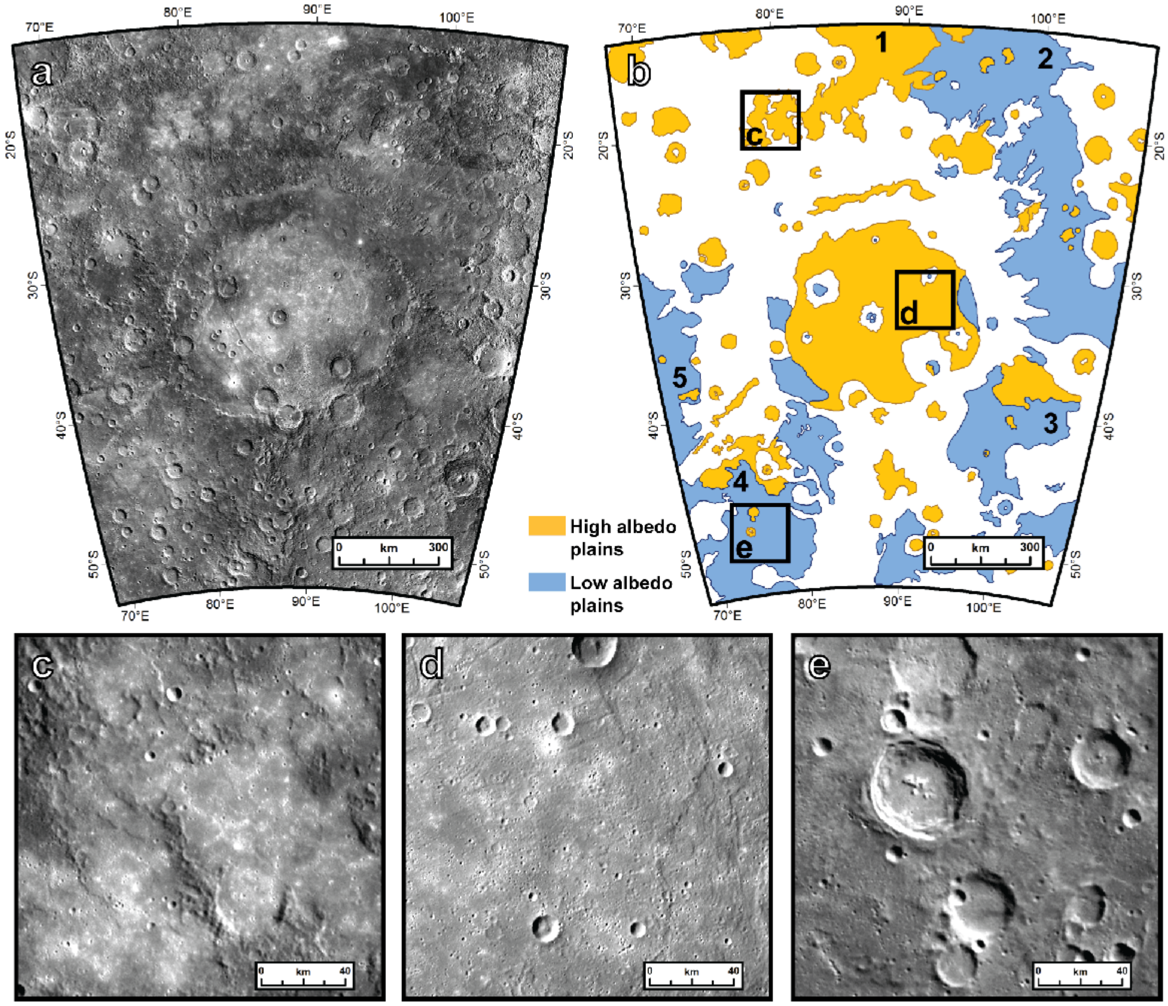

Figure 1. (a) Rembrandt basin. (b) Plains map units both interior and exterior to the basin. High-albedo plains are mapped in orange and low-albedo plains are mapped in blue. Numbers on the mapped plains indicate the areas where crater statistics were compiled. (c-e) Type examples of the mapped plains deposits in part (b). (c) Exterior high-albedo plains; these plains have a smooth surface texture with few superposed impact craters and are brighter than surrounding geologic materials. (d) Interior high-albedo plains; these plains have a morphology and superposed crater population similar to that of the exterior high-albedo plains. (e) Low-albedo exterior plains; these plains appear darker than the surrounding terrain and have a higher density of superposed craters. The surface of low-albedo plains is more textured than either type of high-albedo plains deposit. MDIS 250 m/pixel mosaic. Lambert azimuthal equal area projection centered on Rembrandt basin.